

Final report

Deposition of graphene film as means of injecting charge in diamond-based devices

Nattakarn Suntornwipat, Uppsala University, Uppsala, Sweden

Project summary

The aim of this project is to further optimize the graphene film successfully grown on diamond and to use this as a means to inject charge. The process of depositing graphene is based on rapid thermal annealing in the presence of a metal catalyst. This eliminates the need of transferring graphene to diamond and thus avoids a major challenge in graphene device fabrication. A topological as well as electrical characterization of the graphene layer and how it varies with different parameters is in progress, but further study is still needed.

Background

Diamond is a wide bandgap semiconductor which has many excellent properties such as a high breakdown field, a high thermal conductivity and high carrier mobilities. Together with the possibility to manufacture high quality diamond samples, diamond has become a very interesting material and is a candidate for many electronic devices. The lack of low-ionization-energy dopants is however a big challenge, and by instead depositing a doped semiconductor such as graphene it may be possible to overcome this. Graphene has high carrier mobilities, a high current-carrying capacity, a high saturation velocity and a high thermal conductivity. If the beneficial properties of diamond and graphene were successfully combined, it would give interesting electronic properties suitable for devices used in power electronics and similar fields.

In order to achieve the goals of this project the following questions needed to be addressed:

How can we control the number of graphene layers grown?

Is it enough to change the thickness of the metal catalyst? How does this affect the quality of the film?

How does the annealing temperature and time affect the results?

What can we do to support the experiment results and understand what is going on during the heating process?

Method and Analysis

Over the past nine months this project has led to insights regarding the growth of graphene on diamond. The graphene was deposited using rapid thermal annealing on high-purity SC-CVD diamond samples (3 mm²) supplied by Element Six Ltd, UK. All processing such as varying the metal catalyst thickness, annealing time, annealing temperature etc. and sample characterization were done in-house at Ångström Laboratory, Uppsala.

Copper and nickel are the most frequently used materials for growing graphene but throughout this project we have only focused on nickel. We have previously been successful in applying graphene with nickel as a metal catalyst and without the need of a transferring process. Nickel was directly deposited on the diamond sample using an evaporation process followed by annealing at a high temperature. A wet etch was used to remove the unwanted metal layer and finalize the growth. Raman spectroscopy with an excitation wavelength of 532 nm, X-ray photoelectron spectroscopy (XPS), atomic force microscopy (AFM) and Hall-effect- measurements were used to analyse and characterize the graphene film from both a topological and an electrical perspective.

Summary of Results

Raman spectroscopy together with X-ray photoelectron spectroscopy were used to confirm the occurrence of the graphene layer on top of our diamond samples. **Figure 1** (left) shows the results of the Raman spectrum of a pure diamond sample as well as of a diamond sample with graphene deposited. There are four major peaks at 1334, 1422, 1584, 2703 cm^{-1} which belong to the first order zone-center vibrational mode of diamond, diamond-like carbon species, G peak and 2D peak respectively¹⁻⁵. The full width at half maximum of the 2D peak and the intensity ratio of the 2D and G peaks (I_{2D}/I_G) are $\sim 21 \text{ cm}^{-1}$ and ~ 3.3 , respectively, designating monolayer graphene^{5,6}. A comparison of XPS results between the diamond and the graphene-on-diamond substrate is presented in **Figure 1** (right). Carbon sp^3 hybridization is on the diamond substrate observed at 284.3 eV and a C1s fit with three Gaussian-Lorentzian mix functions on the graphene-on-diamond sample yields peaks at 283.7, 284.3, 285.1 and 286.6 eV. As the distance of the peak at 283.7 eV to that of sp^3 is around 0.6 eV, it is a signature of graphene (sp^2 carbon bonding)⁷⁻⁹. The peaks at 285.1 and 286.6 eV are related to oxidized carbon as oxygen was observed in the survey (as seen in the inset figure).

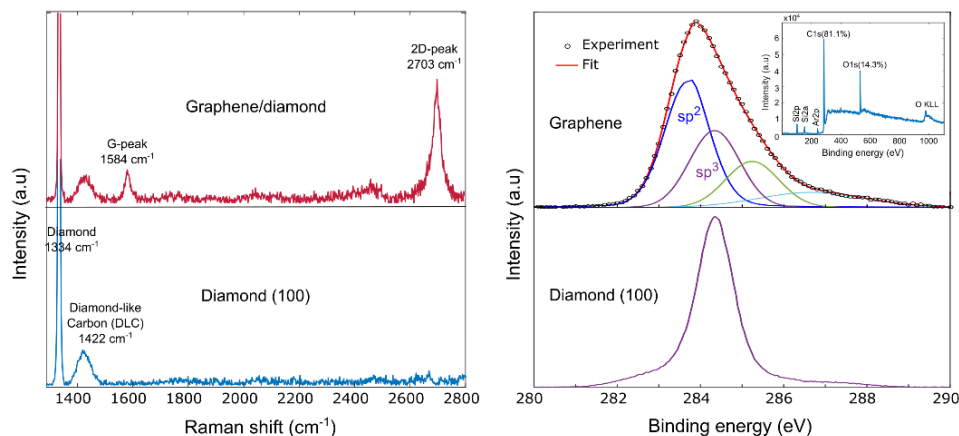


Figure 1: The left figure shows the Raman spectra of diamond and graphene deposited on diamond. The right figure shows XPS results of diamond and graphene deposited on diamond

To perform electrical measurements a two-step standard-lithography process was used to create a Hall-bar structure and 50 nm thick gold contacts on the top of the graphene. Hall-effect measurements were performed at temperatures between 80 and 360 K. The Hall mobility measurement reveals that holes

are the dominating carriers. **Figure 2** shows that the sheet resistivity and the Hall mobility at RT were $3770 \Omega/\square$ and $79 \text{ cm}^2/\text{Vs}$, respectively.

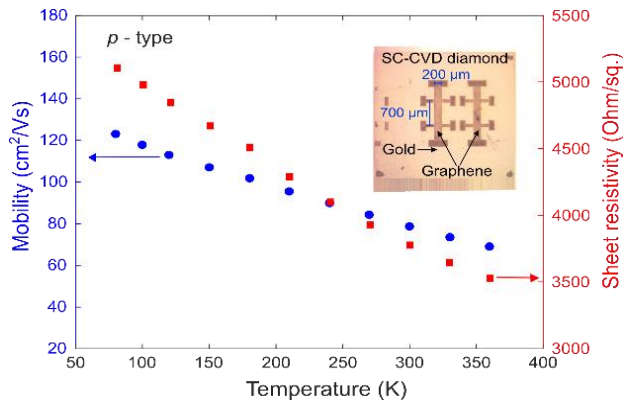


Figure 2: Hall-effect measurements of graphene grown on diamond plotted across different temperatures. The figure shows the sheet resistivity (red squares) and the Hall mobility (blue circles). The inset shows the Hall-bar configuration.

The thickness of the catalyst is one important parameter that influences the graphene growth. A study on Ni thickness deposited on diamond reports that a narrower G- and 2D-peak, corresponding to multilayer graphene, is observed with an increased Ni thickness¹⁰. We investigated Ni thicknesses between 50 and 300 nm with Raman spectroscopy and plotted the ratio between I_{2D} and I_G as probability density functions, as seen in **Figure 3**. A Ni thickness of 50 nm gives the highest ratio ($I_{2D}/I_G \sim 1.39$) with a monolayer coverage estimated to be around 19.8% and a bilayer coverage to be approximately 36.2%.

Furthermore, we have started and will continue to investigate into varying the annealing temperature and time, as well as look into details of the growth by studying the depth profile with XPS. To understand how the graphene grows and the key of initiating the process we recently started a collaboration with another research group where we will compare our experimental results with their simulation.

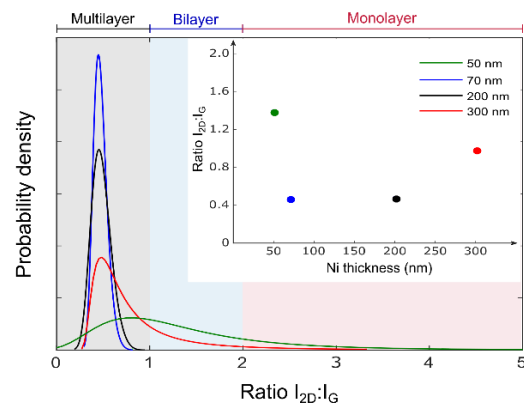


Figure 3: The probability density function of the intensity ratio between I_{2D} and I_G at different Ni thicknesses. The inset shows the average of the probability density of I_{2D}/I_G as a function of Ni thickness.

Outcome

Publications

We currently have a manuscript under review at Diamond Related Material where we are explaining the process used in this project and the results presented here (“*Rapid direct growth of graphene on (100) single-crystalline diamond using nickel as catalyst*”).

Conferences

We presented two posters related to this work at NDNC 2022 in June, named “*Graphene deposition on single crystalline CVD diamond*” presented by me and “*Chemical analysis of carbon atom diffusion through Ni thin film on diamond substrate*” presented by a PhD student in our group.

Conclusion

With the grant awarded for this project we have investigated graphene films grown on a diamond sample and have found the optimal Ni thickness for growing graphene. Even though this has not shown a high hole mobility (*p*-type) we have however observed a higher monolayer coverage than previously reported. We cannot yet control the number of graphene layers, and likely only changing the Ni thickness is not sufficient. We are still investigating how other parameters such annealing temperature and time affect the results. The collaboration will carry on to make sure that we will be able to understand the growth process and hope it could guide us on the correct direction forward.

References

- ¹ R.J. Nemanich, J.T. Glass, G. Lucovsky, and R.E. Shroder, *J. Vac. Sci. Technol. A* **6**, 1783 (1988).
- ² J.J. Chang, T.D. Mantei, R. Vuppuladhadiam, and H.E. Jackson, *Appl. Phys. Lett.* **59**, 1170 (1991).
- ³ K. Ueda, S. Aichi, and H. Asano, *Diam. Relat. Mater.* **63**, 148 (2016).
- ⁴ L.M. Malard, M.A. Pimenta, G. Dresselhaus, and M.S. Dresselhaus, *Phys. Rep.* **473**, 51 (2009).
- ⁵ A. Reina, X. Jia, J. Ho, D. Nezich, H. Son, V. Bulovic, M.S. Dresselhaus, and J. Kong, *Nano Lett.* **9**, 30 (2009).
- ⁶ J. Lee, K.S. Novoselov, and H.S. Shin, *ACS Nano* **5**, 608 (2011).
- ⁷ P.V. Bakharev, M. Huang, M. Saxena, S.W. Lee, S.H. Joo, S.O. Park, J. Dong, D.C. Camacho-Mojica, S. Jin, Y. Kwon, M. Biswal, F. Ding, S.K. Kwak, Z. Lee, and R.S. Ruoff, *Nat. Nanotechnol.* **15**, 59 (2020).
- ⁸ S. Rajasekaran, F. Abild-Pedersen, H. Ogasawara, A. Nilsson, and S. Kaya, *Phys. Rev. Lett.* **111**, 085503 (2013).
- ⁹ T.I.T. Okpalugo, P. Papakonstantinou, H. Murphy, J. McLaughlin, and N.M.D. Brown, *Carbon* **43**, 153 (2005).
- ¹⁰ J.M. García, R. He, M.P. Jiang, P. Kim, L.N. Pfeiffer, and A. Pinczuk, *Carbon* **49**, 1006 (2011).
- ¹¹ M.F. Craciun, S. Russo, M. Yamamoto, and S. Tarucha, *Nano Today* **6**, 42 (2011).